Translational Oncology
www.transonc.com

Volume 7 Number 3 June 2014 pp. 420–428 420

# Promoted Growth of Brain Tumor by the Transplantation of Neural Stem/Progenitor Cells Facilitated by CXCL12[1]

**Nai-Wei Yao*,†, Chiao-Chi V. Chen†, Chen-Tung Yen* and Chen Chang†**

*Department of Life Science, National Taiwan University, Taipei, Taiwan; †Institute of Biomedical Sciences, Academic Sinica, Taipei, Taiwan

## Abstract

The targeted migration of neural stem/progenitor cells (NSPCs) is a prerequisite for the use of stem cell therapy in the treatment of pathologies. This migration is regulated mainly by C-X-C motif chemokine 12 (CXCL12). Therefore, promotion of the migratory responses of grafted cells by upregulating CXCL12 signaling has been proposed as a strategy for improving the efficacy of such cell therapies. However, the effects of this strategy on brain tumors have not yet been examined *in vivo*. The aim of the present study was thus to elucidate the effects of grafted rat green fluorescent protein (GFP)–labeled NSPCs (GFP-NSPCs) with CXCL12 enhancement on a model of spontaneous rat brain tumor induced by *N*-ethyl-*N*-nitrosourea. $T_2$-weighted magnetic resonance imaging was applied to determine the changes in tumor volume and morphology over time. *Postmortem* histology was performed to confirm the tumor pathology, expression levels of CXCL12 and C-X-C chemokine receptor type 4, and the fate of GFP-NSPCs. The results showed that the tumor volume and hypointense areas of $T_2$-weighted images were both significantly increased in animals treated with combined NSPC transplantation and CXCL12 induction, but not in control animals or in those with tumors that received only one of the treatments. GFP-NSPCs appear to migrate toward tumors with CXCL12 enhancement and differentiate uniquely into a neuronal lineage. These findings suggest that CXCL12 is an effective chemoattractant that facilitates exogenous NSPC migration toward brain tumors and that CXCL12 and NSPC can act synergistically to promote tumor progression with severe hemorrhage.

*Translational Oncology (2014) 7, 420–428*

## Introduction

It has been shown that transplantation of neural stem/progenitor cells (NSPCs) has potential as a therapy for various disorders of the central nervous system, such as stroke [1], multiple sclerosis [2], Parkinson disease [3], Huntington disease [4], amyotrophic lateral sclerosis [5], and gliomas [6–9]. NSPCs tend to migrate toward injured regions in these various brain pathologies [1,2,4,7–9]; this migration is regulated mainly by the signaling axis of C-X-C motif chemokine 12 (CXCL12) and its receptor C-X-C chemokine receptor type 4 (CXCR4) [10]. NSPCs move along the CXCL12 concentration gradient formed by the increased levels at sites of injuries [11–13], resulting in targeted migration [10,13–15].

Targeted migration of NSPCs to lesion sites is essential for the direct repair of damaged tissues. Therefore, the promotion of that migratory behavior through manipulation of CXCL12 signaling has been proposed as a therapeutic strategy, whereby transplanted cells would facilitate recovery processes [15–20]. In support of this, treatments that block CXCL12 signaling were found to result in a marked impairment of migration and proliferation of the engrafted NSPCs [14]. Furthermore, locally administered CXCL12 stimulates the recruitment of stem/progenitor cells, which promotes

Address all correspondence to: Chen-Tung Yen, PhD, Department of Life Science, National Taiwan University, No. 1, Sec 4, Roosevelt Road, Taipei 10617, Taiwan or Chen Chang, PhD, Institute of Biomedical Sciences, Academia Sinica, 128 Sec 2, Academia Road, Nankang, Taipei 11529, Taiwan. E-mail: ctyen@ntu.edu.tw, bmcchen@ibms.sinica.edu.tw

[1] This study was supported by the National Science Council, Taiwan (grants NSC98-2314-B-001-002-MY3 and NSC101-2320-B-001-036-MY3). The funders had no role in the study design, data collection and analysis, decision to publish, or preparation of the manuscript. The authors have no conflicts of interest to declare.
Received 18 December 2013; Revised 10 April 2014; Accepted 14 April 2014


1936-5233/14
http://dx.doi.org/10.1016/j.tranon.2014.04.007

repair in stroke [15] and ischemic lesions [20], functional improvement of Alzheimer disease [19], skeletal regeneration [16], and wound healing [17].

The first clear demonstration that NSPCs could exhibit migratory activity toward the site of a brain tumor was provided by Aboody and colleagues [9]. NSPCs have the potential to specifically target the sites of brain tumors [9] and could thus be used as therapeutic vehicles [21]. If the targeted migration of NSPCs could be accelerated by promoting CXCL12 signaling, this would make NSPCs particularly useful in cell-based brain tumor therapy. However, the strategy of promoting migratory behavior in brain tumors by the manipulation of CXCL12 signaling has not been examined *in vivo* previously. To assess the effects of this strategy on brain tumors, this study used magnetic resonance imaging (MRI) to monitor the pathologic changes of brain tumors *in vivo* following combined treatment with NSPC implantation and CXCL12 facilitation.

The effects of treatments on the natural development of glioma were investigated using a model of spontaneous brain tumor in which rats develop various gliomas several months after transplacental administration of *N*-ethyl-*N*-nitrosourea (ENU) as described previously [22–24]. Furthermore, the immune rejection responses of the xenografts [25] were minimized by using the same species of NSPCs as that used in the ENU-induced rat brain tumor model. The tumorigenic potential of immortalized cells [26–28] was avoided by applying NSPCs from primary cultures. The locations of cells were determined by injecting green fluorescent protein (GFP)–expressing NSPCs (GFP-NSPCs) from GFP-expressing transgenic rats intraventricularly into the brain of tumor-bearing rats. Simultaneously, these rats received an intracerebral injection of CXCL12 near to the tumor sites to promote NSPC migration.

MRI was applied because it allows repeated imaging with a high spatial resolution; MRI can provide accurate tumor volume measurements and morphologic information over longitudinal time points and can thus be used to evaluate the effects of cell therapies [29]. $T_2$-weighted MRI images ($T_2$WIs) were acquired to measure tumor volumes and monitor the tumor morphology [30] for 42 days after surgery. $T_2$WIs further confirmed the histologic features of the gliomas following the treatments. The findings of this study suggest that CXCL12 is an effective chemoattractant that facilitates the tumor-targeted migration of exogenous NSPCs and that CXCL12 and NSPC can act synergistically to promote tumor progression with severe hemorrhage.

## Materials and Methods

### *Animals*

Eleven pregnant Sprague-Dawley rats (the National Laboratory Animal Center of Taiwan, Taipei, Taiwan) and 27 of their 118 offspring were used for the tumor model in this study. In total, 70 neonatal GFP-expressing transgenic rats ("green rat" CZ-004, SD-Tg(Act-EGFP) CZ-004Osb; Japan SLC, Shizuoka, Japan) were used for harvesting the primary NSPCs. The animals were housed in a well-controlled environment with a 12-hour/12-hour light/dark cycle and controlled humidity and temperature. Rats were triple housed in plastic cages with *ad libitum* access to food and water. All experimental procedures were approved by the Institute of Animal Care and Utilization Committee at Academia Sinica (Taipei, Taiwan).

### *The ENU-Induced Brain Tumor Model*

The pregnant Sprague-Dawley rats were placed into a restrainer and injected intraperitoneally with 50 mg/kg ENU (Sigma-Aldrich, St Louis, MO) at 18 days of gestation using a 26-gauge needle for several minutes. MRI was applied to 120-day-old offspring to confirm the location and size of the tumors. Rats with similar-sized tumors (~1 $mm^3$) near the corpus callosum were selected for experiments. Rats with trigeminal neurinoma and pituitary tumors or with obvious physiological defects were excluded from this study.

### *Harvesting and Culturing of Primary GFP-NSPCs*

GFP-NSPCs were harvested from both lateral walls of the ventricle in neonatal GFP-expressing transgenic rats and cultured as described elsewhere [31,32]. In brief, pooled tissues isolated from the lateral walls were dissociated by mechanical trituration in NSPC medium, which consists of Dulbecco's modified Eagle's medium/F12 (Invitrogen/Gibco BRL, Grand Island, NY) with 0.3% glucose, 23 μg/ml insulin, 92 μg/ml apotransferrin, 55 μM putrescine, 25 nM sodium selenite, 6.28 ng/ml progesterone, 20 ng/ml epidermal growth factor, and 20 ng/ml fibroblast growth factor. The cells were then counted and plated at a density of $1.5 \times 10^6$ cells in T75 flasks (Orange Scientific, Brussels, Belgium) with 20 ml of medium. The cultures were replenished with 20 ml of NSPC medium every 2 days. The cultures were maintained at 37°C in a humidified atmosphere of 5% $CO_2$/95% air. At 5 to 7 days after isolation, the cells grew as free-floating neurospheres, which were dissociated into single cells for transplantation when they reached diameters of 140 to 160 μm.

### *GFP-NSPC Implantation and Local CXCL12 Administration*

The rats were randomly assigned to the following treatment groups: 1) NSPC only ($n$ = 6), 2) CXCL12 only ($n$ = 6), 3) CXCL12-NSPC ($n$ = 6), and 4) sham ($n$ = 6). The animals were anesthetized with chloral hydrate (450 mg/kg; Sigma-Aldrich) and positioned in a stereotaxic apparatus. In the case of GFP-NSPC transplantation (i.e., NSPC and CXCL12-NSPC groups), the cells were freshly prepared [$1 \times 10^6$ in 5 μl of phosphate-buffered saline (PBS), pH 7.4] and implanted into the lateral ventricle ipsilateral to the site of tumors (bregma = –0.5 mm; lateral = –1.5 or 1.5 mm; and depth = 3.5 mm) using a 10-μl Hamilton syringe with a 30S-gauge needle at a rate of 0.5 μl/min. The following doses of CXCL12 (Sigma-Aldrich) had been tested in a pilot study: 0.2, 1, and 2 μg/μl. The tumor promotion effect was greater for tumors treated with 1 μg/μl CXCL12 and NSPCs, and hence, 1 μg/μl CXCL12 in 5 μl of PBS (pH 7.4) was selected for use in this study. In the CXCL12-NSPC and CXCL12-only groups, a solution of CXCL12 was injected stereotaxically near the tumor sites using the same surgical procedure as described above.

### *Magnetic Resonance Imaging*

The animals underwent five MRI examinations, with the same imaging procedure being followed for every time point. Images were acquired at 0, 1, 14, 28, and 42 days after injections (no data are shown herein for the 1-day time point). All MRI examinations were performed using a horizontal 7.0-T spectrometer (PharmaScan 70/16; Bruker, Ettlingen, Germany) with an active shielding gradient of 300 mT/m in 80 microseconds. The animals were anesthetized with 2% isoflurane in $O_2$ at a flow rate of 1 l/min. The breathing rate was maintained at between 60 and 70 breaths per minute. The

anesthetized rats were fitted into a custom-designed head holder and immobilized with ear bars to minimize movement artifacts. $T_2$WIs were acquired with the following parameters: field of view = 3 cm; slice thickness = 1 mm; 28 slices; repetition time = 5100 milliseconds; echo time = 70 milliseconds; echo train length = 8; number of excitations = 6; and matrix size = 256 × 256. These images were used to measure the tumor volume and to monitor the tumor morphology.

### *Data Analysis*

The outlines of the tumors were delineated on the basis of the contrast provided by the $T_2$WIs between the tumor and the brain tissues. The total tumor volume was calculated by summing the tumor area in three dimensions using Avizo software (version 6.0; Visualization Sciences Group, Burlington, MA). Growth curves were plotted as the change in tumor volume at each time point relative to the baseline volume. The hypointense area was selected manually on the $T_2$WIs. The total hypointense volume was calculated by summing the hypointense areas in three dimensions using Avizo software. The ratio of the intratumoral hypointense area was then calculated by dividing the intratumoral hypointense volume by that of the entire tumor region.

### *Histologic Examination*

To correlate MRI signal changes with histologic data, animals were perfused transcardially with 4% paraformaldehyde (Sigma-Aldrich) in PBS (pH 7.4) immediately after the scanning performed at the last time point. The brains were removed from the cranium, kept in the same fixative overnight at 4°C, and then sectioned at a thickness of 50 μm using a cryostat (CM 3050S; Leica Microsystems, Wetzlar, Germany). The brain sections were stained using hematoxylin and eosin (H&E) to confirm whether the signal changes detected on the $T_2$WIs were indeed induced by the pathologic conditions, such as necrosis and hemorrhage within the tumor. Primary antibodies raised against CXCL12 (Santa Cruz Biotechnology, Santa Cruz, CA), CXCR4 (Santa Cruz Biotechnology),

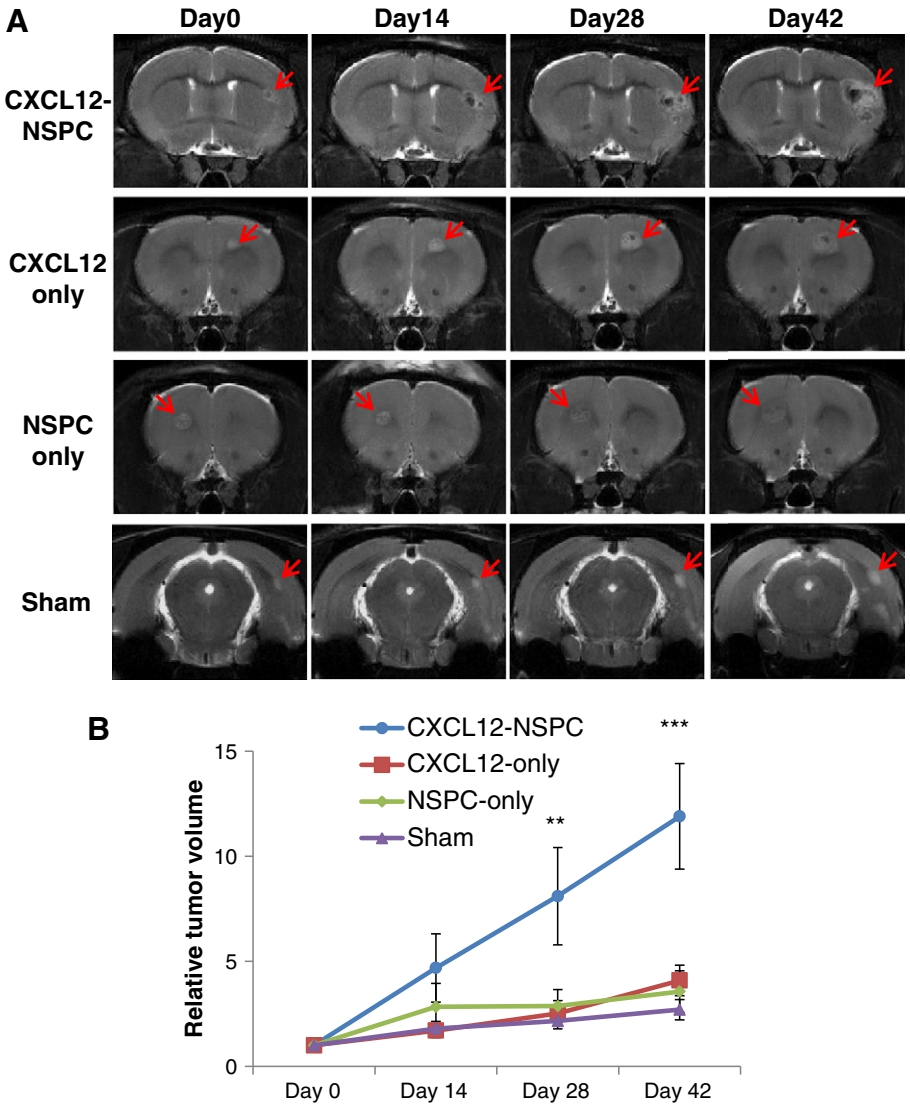


**Figure 1.** The combination of CXCL12 elevation and GFP-NSPC transplantation promoted ENU-induced brain tumor growth. (A) A series of representative axial $T_2$WIs from the CXCL12-NSPC ($n$ = 6), CXCL12-only ($n$ = 6), NSPC-only ($n$ = 6), and sham ($n$ = 6) groups acquired on days 0, 14, 28, and 42 after tumor detection is shown. Red arrows indicate the tumor location. (B) Tumor growth curve. On days 28 and 42, the tumor volume was significantly greater in the CXCL12-NSPC group than those in each of the other groups (**$P$ < .01 and ***$P$ < .001).

GFP (Chemicon International, Temecula, CA), and NeuN (Chemicon International) were used to examine the expression patterns of the chemokine and its receptor and the location of GFP-NSPCs and to confirm the neuronal lineage of the GFP-NSPCs.

Due to high tissue autofluorescence, two chromogens—nickel-intensified DAB and DAB—were used for immunohistochemistry in this study. Free-floating sections were treated with 0.2% $H_2O_2$ in PBS containing 0.3% Triton X-100 to inhibit endogenous peroxidase staining. Nonspecific binding was blocked by incubating sections in blocking solutions for 1 hour. BSA was used at specific concentrations in PBS with 0.3% Triton X-100 as the blocking solution for the various primary antibodies: 1% BSA for CXCL12, 3% BSA for CXCR4 and GFP, and 1.2% BSA for NeuN. The sections were subsequently incubated with diluted primary antibodies (1:200 for CXCL12, 1:200 for CXCR4, 1:1000 for GFP, and 1:400 for NeuN) overnight at room temperature, washed in PBS with 0.3% Triton X-100, and then placed into solutions of the corresponding biotinylated secondary antibodies (1:500, goat anti-rabbit antibody or donkey anti-goat antibody; Jackson ImmunoResearch Laboratories, West Grove, PA) for 1 hour. After washing, the sections were exposed to avidin-biotin-peroxidase complex (1:500; ABC Elite kit; Vector Laboratories, Burlingame, CA) for 1 hour at room temperature and then stained with 0.025% DAB, 1.5% nickel ammonium sulfate, and 0.024% $H_2O_2$ in PBS for 5 to 10 minutes until the desired dark-purple coloration had developed. To double-stain with GFP, the same procedures were employed for sections with NeuN staining as described above but without the 1.5% nickel ammonium sulfate in the development step, resulting in the development of a brown coloration. The sections were then washed, mounted on coated slides, dehydrated, and coverslipped with dibutyl phathalate xylene (DPX) mounting solution (Sigma-Aldrich).

### *Statistical Analysis*

All data are presented as mean ± SEM values. Between-group differences in tumor volume, the ratio of hypointense areas, and numbers of GFP-positive ($GFP^+$) cells and $GFP^+$/NeuN-positive ($NeuN^+$) cells were tested with analysis of variance, followed by Fisher *post hoc* tests. All statistical analyses were performed using

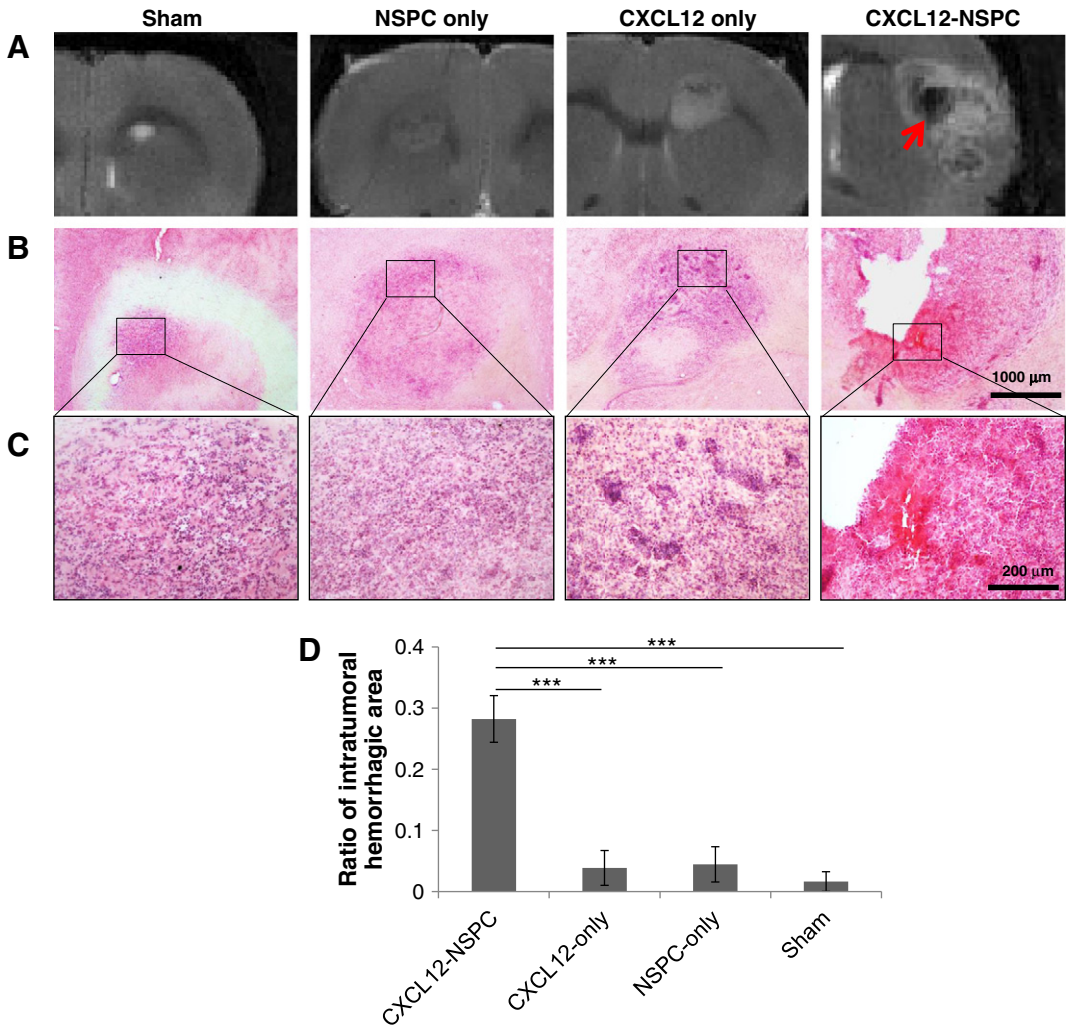


**Figure 2.** A significant increase in the degree of intratumoral hemorrhage was found in tumors from brains treated with the combination of CXCL12 and GFP-NSPCs. (A) In $T_2$WIs, severe signal loss (red arrow) was found in tumors from the CXCL12-NSPC group on day 42. (B) H&E staining was used to confirm the source of the changes in MRI signal in the tumor tissue. (C) Enlarged views of H&E-stained sections are shown. (D) The ratio of intratumoral hemorrhagic area was significantly higher in the CXCL12-NSPC group than in all other groups (***$P < .001$).

StatView software (SAS Institute, Cary, NC). The level of statistical significance was set at $P < .05$.

## Results

### *The Combination of CXCL12 and GFP-NSPCs Promotes ENU-Induced Brain Tumor Growth*

Tumor volumes were determined by analyzing $T_2$WIs at 0, 14, 28, and 42 days after injections (Figure 1*A*). The curves of relative tumor growth show that the tumors in the CXCL12-NSPC group grew faster than those in all other groups (Figure 1*B*). At days 28 and 42, the relative tumor volume was significantly larger in the CXCL12-NSPC group than in the other groups (Figure 1*B*) and did not differ significantly among the CXCL12-only, NSPC-only, and sham groups at any of the time points [analysis of variance: $F(6,40) = 14.5$, $P < .0001$; Fisher *post hoc* tests: all $P$ values $< .01$ for CXCL12-NSPC *vs* any of the other groups at day 28 and all $P$ values $< .001$ for CXCL12-NSPC *vs* any of the other groups at day 42]. A limited effect was found when either CXCL12 or GFP-NSPCs were given alone, but a significant degree of tumor promotion in ENU-induced brain tumors was only found after administration of the combination of CXCL12 and GFP-NSPCs.

### *The Combination of CXCL12 and GFP-NSPCs Increases the Severity of Intratumoral Hemorrhage*

Severe signal loss on $T_2$WI was observed in tumors of the CXCL12-NSPC group on day 42 but not in the tumors of the other groups (Figure 2*A*). H&E staining indicated that this signal loss was attributable to intratumoral hemorrhage (Figure 2*B*). As shown in Figure 2*C* (magnified views of Figure 2*B*), an extensive area of hemorrhage (bright pink color on H&E staining) is clearly observed in the CXCL12-NSPC group. The hypointense areas were measured, and the ratios of the intratumoral hypointense areas were then calculated (Figure 2*D*). The ratio of the hypointense area to that of the entire tumor region was significantly higher in the CXCL12-NSPC group than in the other groups ($P < .001$).

### *Increased CXCL12 and CXCR4 Expression Following Combined GFP-NSPC and CXCL12 Treatments*

The expression levels of CXCL12 and CXCR4 in the tumors of the four treatment groups were examined by immunohistochemistry (Figure 3). Strong CXCL12 and CXCR4 expressions were detected in the CXCL12-NSPC group (Figure 3, CXCL12 and CXCR4). In addition, moderate CXCL12 and slight CXCR4 expressions were observed in the CXCL12-only group. The expression levels of CXCL12 and CXCR4 were either low or undetectable in the NSPC-only and sham groups.

### *Histologic Evidence of GFP-NSPC–Targeted Migration into the Glioma Region*

The grafted GFP-NSPCs in the brains of animals in the CXCL12-NSPC and NSPC-only groups were identified by immunohistochemistry (Figure 4*A*, GFP). No GFP immunoreactivity was found in

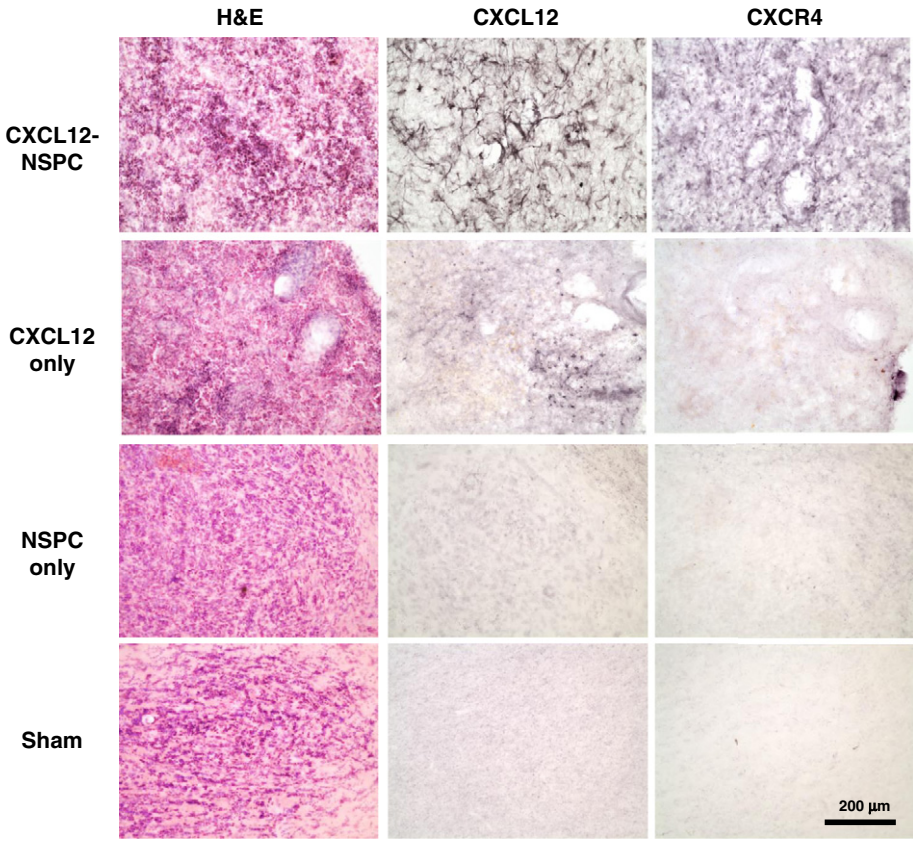


**Figure 3.** Immunohistochemical staining for CXCL12 and CXCR4 in tumors from the four treatment groups. CXCL12 and CXCR4 immunoreactivities were both strong in tumors from the CXCL12-NSPC group, moderate in those from the CXCL12-only group, and undetectable in the NSPC-only and sham groups.

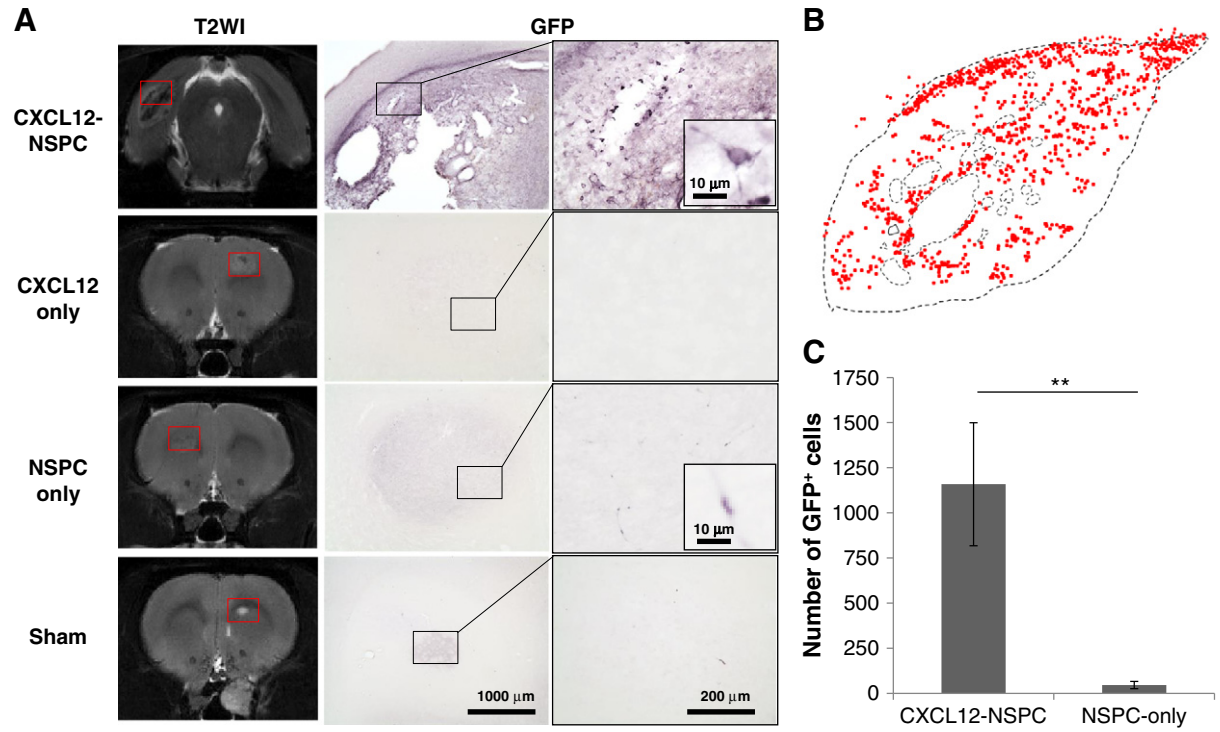


**Figure 4.** Numerous GFP-NSPCs were found in the CXCL12-NSPC group. (A) GFP immunohistochemical staining was employed in tissue samples obtained from all treatment groups to identify the locations of the GFP-NSPCs. (B) Diagrammatic representation of the distribution of $GFP^+$ cells in the CXCL12-NSPC group. The grafted cells were found on the tumor border and in the tumor mass. (C) The number of $GFP^+$ cells was significantly greater in the CXCL12-NSPC group than in the NSPC-only group (**$P < .01$).

the CXCL12-only and sham groups, as expected, because GFP-NSPC transplantation was not employed in these groups. $GFP^+$ cells were widespread in the tumors of the CXCL12-NSPC group, but only a few $GFP^+$ cells were observed in the tumors of the NSPC-only group. A representative diagram of the distribution of $GFP^+$ cells in the tumors of the CXCL12-NSPC group is shown in Figure 4*B*, in which each red dot represents two or three $GFP^+$ cells. The number of $GFP^+$ cells that had migrated toward tumor sites differed significantly between the CXCL12-NSPC (1159 ± 341 cells) and NSPC-only (45.7 ± 19.8 cells) groups ($P < .01$; Figure 4*C*).

### *Phenotypic Characterization of GFP-NSPCs*

The grafted cells identified by GFP staining exhibited neuronal-like morphology with extended neurites (Figure 4*A*, magnified images from the CXCL12-NSPC and NSPC-only groups). Double labeling with NeuN (which is a neuronal marker) and GFP was employed to

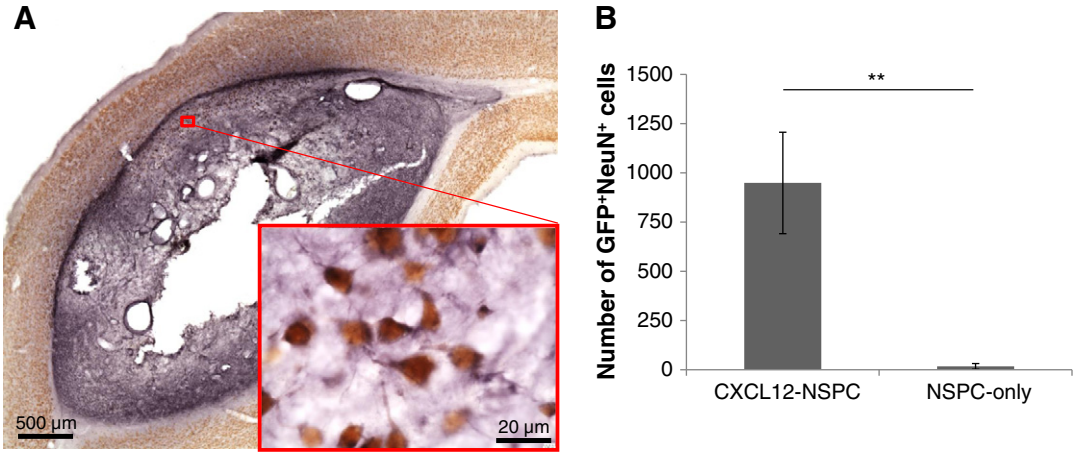


**Figure 5.** Neuronal phenotype of the GFP-NSPCs in the CXCL12-NSPC group. (A) Double immunohistochemical staining of GFP and NeuN. Light microscopy of double immunohistochemical staining for GFP (dark purple) and the neuronal marker NeuN (brown) demonstrates that most of the cells express both GFP and NeuN. (B) The number of $GFP^+/NeuN^+$ cells differed significantly between the CXCL12-NSPC and NSPC-only groups (**$P < .01$).

**Table 1.** Numbers of GFP⁺/NeuN-Negative (NeuN⁻), GFP⁺/NeuN⁺, and GFP-Negative (GFP⁻)/NeuN⁺ Cells in the CXCL12-NSPC and NSPC-Only Groups.

| | | No. of Cells | |
|---|---|---|---|
| | | CXCL12-NSPC | NSPC Only |
| GFP⁺ | GFP⁺/NeuN⁻ | 209.8 ± 107.8 | 28.7 ± 16.2 |
| | GFP⁺/NeuN⁺ | 948.7 ± 257.7 | 17.0 ± 14.6 |
| GFP⁻ | *GFP⁻/NeuN⁺ | 244.2 ± 81.9 | 13.7 ± 12.3 |

* Few GFP⁻/NeuN⁺ cells were found in the CXCL12-only and sham groups (data not shown).

confirm the neuronal lineage of these GFP⁺ cells (Figure 5*A*). GFP⁺/NeuN⁺ double staining demonstrated that ~80% of the GFP⁺ cells expressed NeuN in the tumors of the CXCL12-NSPC group (see Table 1). The number of GFP⁺/NeuN⁺ cells in the tumor regions (Figure 5*B*) differed significantly between the CXCL12-NSPC (949 ± 258 cells) and NSPC-only (17.0 ± 14.6 cells) groups ($P < .01$; Figure 5*B*). Only a few NeuN⁺ cells were found in the CXCL12-only and sham groups (data not shown).

## Discussion

The targeted migration of stem cells is essential for the direct repair of injured tissues. Several studies have found that a strategy involving promoting CXCL12, which is a major signaling factor in NSPC migration, enhanced the migration of transplanted cells toward lesion sites [15–20]. The effects of this strategy on brain tumors had not been examined previously; the present study has demonstrated that this strategy elicits a striking tumor-promoting effect. The local administration of CXCL12 boosts the CXCL12-directed migration of grafted NSPCs toward the sites of ENU-induced brain tumors. However, enhanced tumor outgrowth and increased intratumoral hemorrhage were found in tumors receiving the combined CXCL12-NPSC treatment (Figures 1 and 2). Accordingly, under CXCL12 facilitation, NSPC may play a role in promoting tumor progression.

The role of NSPCs in brain tumor growth remains controversial. There are reports that unmodified and endogenous neural precursors can inhibit tumor outgrowth [6,33]. However, the potential of NSPC transformation [34,35] and their involvement in tumor development [36] have long been considered. Clinically, it has also been shown that gliomas covering the subventricular zone had a worse prognosis for patients, indicating the tumorigenic potential of NSPCs [37,38]. These findings suggest that NSPCs exert adverse effects under certain circumstances.

Hemorrhage is a rupture of blood vessels that results in the release of blood cells and other blood-borne substances into the surrounding tissues. Intratumoral hemorrhage is commonly seen in malignant brain tumors, and the etiology of hemorrhage has been attributed to factors such as hypervascularity, abundant microvessel proliferation, unstable vascular structures, blood-brain barrier disruption, and necrosis with release of intracellular proteolytic enzymes due to rapid tumor growth [39]. Necrosis of the tumor can cause a direct breakdown of vessels in the tumor regions including pre-existing and newly formed vessels and subsequent hemorrhage [40]. The results of H&E staining strongly suggest that hypointense areas are attributable to intratumoral hemorrhage (Figure 2). The present study found a significant increase in intratumoral hemorrhage in tumors that had received the combined CXCL12-NPSC treatment (Figure 2), illustrating the potential role of this strategy in rapid tumor progression, which eventually causes necrosis and intratumoral hemorrhage. Compared to all other groups, tumors in the CXCL12-NSPC group exhibited the largest hemorrhagic areas and the highest level of CXCL12 (Figures 2 and 3). CXCL12 induces basement membrane degradation [41], promotes proliferation of endothelial [42] and glioma [43] cells, and increases the permeability and disruption of the blood-brain barrier [44], suggesting that the level of CXCL12 is closely associated with the grade of hemorrhage.

Stronger migratory responses of NSPCs were associated with higher levels of chemokine at targeted sites. CXCL12 may have formed a strong gradient that attracted a large number of grafted NSPCs toward tumors of the CXCL12-NSPC group (Figure 4). In addition, CXCL12 may promote the survival of NSPCs as an alternative explanation for why more of these cells were detected in the combined treatment group [45]. No therapeutic effect of NSPC transplantation alone on brain tumors was observed in the present study. This may be due to only a few NSPCs migrating toward sites of ENU-induced brain tumors with low or undetectable CXCL12 levels to exert tumor-inhibitory functions (Figure 3). Stronger CXCL12 and CXCR4 expressions were detected in the CXCL12-NSPC group than in the CXCL12-only group (Figure 3, CXCL12 and CXCR4), which may have resulted from the interaction between NSPCs and CXCL12. When the level of CXCL12 is high, it has been shown to act synergistically with NSPCs [46,47] to upregulate CXCL12/CXCR4 signaling of astrocytes [48], endothelial cells [49,50], and tumor cells [51]. The scarce CXCR4 expression in the CXCL12-only group is probably attributable to CXCL12 alone at the given dose not forming a gradient that was sufficiently strong to attract CXCR4-expressing cells toward tumor sites. In contrast, the combination of CXCL12 and NSPC exerted significant effects in recruiting CXCR4-expressing cells into the tumor, thereby elevating CXCR4 levels at the tumor site. Furthermore, CXCL12 not only elicits migratory responses but also increases the proliferation [10] and CXCR4 expression [46] of grafted NSPCs. The grafted NSPCs would be activated by CXCL12, and the NSPCs may tend to be closely associated with endothelial cells and astrocytes (which express CXCR4), which would support their survival and growth [10,52,53]. This is another possible source of the CXCR4 expression seen in the CXCL12-NSPC group.

The chemokine CXCL12 and its cell surface receptor CXCR4 are vital mediators of NSPC migration toward brain tumors. Murine NSPCs inoculated into established intracranial GL26 tumors have demonstrated significant tumor-specific migration away from the site of inoculation to the proximity of the disseminating tumor cells [54]. Cells that had demonstrated tumor-tracking behavior showed significant staining for CXCR4. In the same study, both murine and human fetal NSPC migration toward tumor-conditioned medium could be impaired by using anti-CXCL12 and anti-CXCR4 neutralizing antibodies. Intravascularly injected murine NSPCs have been shown to migrate to and infiltrate subcutaneous and intracranial glioma tumors in nude mice [55]. CXCL12 expressed by a tumor-derived endothelium may attract NSPCs to migrate to the site of the tumor [53,56]. Furthermore, NSPC-to-glioma tropism was increased through up-regulation of CXCR4 on NSPCs and CXCL12 on glioma cells under a hypoxic condition [57]. All of these findings indicate the importance of CXCL12 and CXCR4 in the tumor-specific migration of NSPCs.

The fate of grafted NSPCs in the brain tumors is for them to remain in a quiescent and undifferentiated state [9,58,59]. However, contrary to these previous reports, most of the grafted cells migrating to tumors with CXCL12 facilitation in the present study were found

to differentiate into neurons (Figure 5 and Table 1). Two possible reasons for the contradictory findings are the species from which the NSPCs originated (rat in this study and human or mouse in the aforementioned studies) and the high levels of CXCL12 used in the present study. Unlike mouse and human NSPCs, which can be maintained for a long period of time *in vitro* without genetic modifications, rat NSPCs derived from the subventricular zone or hippocampal subgranular zone typically sustain proliferation for only a relatively short time and have a tendency to differentiate [60,61]. In addition, local administration of CXCL12 may create a distinct local environment that stimulates NSPCs to differentiate into neurons. CXCL12 was shown to promote neuronal survival and the differentiation of NSPCs to support neural tissues [15,62] and to stimulate neurite outgrowth and axonal branching of cultured neuronal cells [63,64], indicating its role in controlling neuronal differentiation. Together, these results indicate that rat NSPCs, which tend to differentiate, may respond to CXCL12 induction and, as a result, differentiate into neurons.

It has recently been reported that the expressions of neuronal markers in brain tumors may be associated with a poor outcome [65–67]. NeuN was noted to be present in various types of high-grade and recurrent gliomas [65,66]. Multiple neuronal immunomarker expressions in glioma were associated with a poor survival rate [67]. We have demonstrated herein that ~80% of grafted cells migrating toward tumors with the combined CXCL12-NPSC treatment differentiated into neurons (Figures 4 and 5). The present results show that the increased number of neurons in tumors was associated with increased tumor volume. However, the roles of such an increased number of tumor neurons remain unclear.

The strategy of using exogenous CXCL12 to promote NSPC migration in brain tumors was found in the present study to be associated with a higher rate of tumor growth and an increase in intratumoral hemorrhage. These grafted NSPCs that migrated toward the tumors tended to differentiate into neurons due to the known differentiation potential of rat NSPCs and induction by CXCL12. In conclusion, the results of the present study are especially important in that they illustrate possible effects of stem cell therapies on brain tumors. That is, the strategy of further promoting targeted NSPC migration by CXCL12 may lead to adverse effects.

## References


[1] Darsalia V, Kallur T, and Kokaia Z (2007). Survival, migration and neuronal differentiation of human fetal striatal and cortical neural stem cells grafted in stroke-damaged rat striatum. *Eur J Neurosci* **26**, 605–614.

[2] Einstein O, Karussis D, Grigoriadis N, Mizrachi-Kol R, Reinhartz E, Abramsky O, and Ben-Hur T (2003). Intraventricular transplantation of neural precursor cell spheres attenuates acute experimental allergic encephalomyelitis. *Mol Cell Neurosci* **24**, 1074–1082.

[3] Ourednik J, Ourednik V, Lynch WP, Schachner M, and Snyder EY (2002). Neural stem cells display an inherent mechanism for rescuing dysfunctional neurons. *Nat Biotechnol* **20**, 1103–1110.

[4] Lee ST, Chu K, Park JE, Lee K, Kang L, Kim SU, and Kim M (2005). Intravenous administration of human neural stem cells induces functional recovery in Huntington's disease rat model. *Neurosci Res* **52**, 243–249.

[5] Corti S, Locatelli F, Papadimitriou D, Del Bo R, Nizzardo M, Nardini M, Donadoni C, Salani S, Fortunato F, and Strazzer S, et al (2007). Neural stem cells LewisX+CXCR4+ modify disease progression in an amyotrophic lateral sclerosis model. *Brain* **130**, 1289–1305.

[6] Staflin K, Honeth G, Kalliomäki S, Kjellman C, Edvardsen K, and Lindvall M (2004). Neural progenitor cell lines inhibit rat tumor growth *in vivo*. *Cancer Res* **64**, 5347–5354.

[7] Li S, Gao Y, Tokuyama T, Yamamoto J, Yokota N, Yamamoto S, Terakawa S, Kitagawa M, and Namba H (2007). Genetically engineered neural stem cells migrate and suppress glioma cell growth at distant intracranial sites. *Cancer Lett* **251**, 220–227.

[8] Brekke C, Williams SC, Price J, Thorsen F, and Modo M (2007). Cellular multiparametric MRI of neural stem cell therapy in a rat glioma model. *Neuroimage* **37**, 769–782.

[9] Aboody KS, Brown A, Rainov NG, Bower KA, Liu S, Yang W, Small JE, Herrlinger U, Ourednik V, and Black PM, et al (2000). Neural stem cells display extensive tropism for pathology in adult brain: evidence from intracranial gliomas. *Proc Natl Acad Sci U S A* **97**, 12846–12851.

[10] Imitola J, Raddassi K, Park KI, Mueller FJ, Nieto M, Teng YD, Frenkel D, Li J, Sidman RL, and Walsh CA, et al (2004). Directed migration of neural stem cells to sites of CNS injury by the stromal cell-derived factor 1α/CXC chemokine receptor 4 pathway. *Proc Natl Acad Sci U S A* **101**, 18117–18122.

[11] Hill WD, Hess DC, Martin-Studdard A, Carothers JJ, Zheng J, Hale D, Maeda M, Fagan SC, Carroll JE, and Conway SJ (2004). SDF-1 (CXCL12) is upregulated in the ischemic penumbra following stroke: association with bone marrow cell homing to injury. *J Neuropathol Exp Neurol* **63**, 84–96.

[12] Miller JT, Bartley JH, Wimborne HJ, Walker AL, Hess DC, Hill WD, and Carroll JE (2005). The neuroblast and angioblast chemotaxic factor SDF-1 (CXCL12) expression is briefly up regulated by reactive astrocytes in brain following neonatal hypoxic-ischemic injury. *BMC Neurosci* **6**, 63.

[13] Robin AM, Zhang ZG, Wang L, Zhang RL, Katakowski M, Zhang L, Wang Y, Zhang C, and Chopp M (2006). Stromal cell-derived factor 1α mediates neural progenitor cell motility after focal cerebral ischemia. *J Cereb Blood Flow Metab* **26**, 125–134.

[14] Carbajal KS, Schaumburg C, Strieter R, Kane J, and Lane TE (2010). Migration of engrafted neural stem cells is mediated by CXCL12 signaling through CXCR4 in a viral model of multiple sclerosis. *Proc Natl Acad Sci U S A* **107**, 11068–11073.

[15] Shyu WC, Lin SZ, Yen PS, Su CY, Chen DC, Wang HJ, and Li H (2008). Stromal cell-derived factor-1 α promotes neuroprotection, angiogenesis, and mobilization/homing of bone marrow-derived cells in stroke rats. *J Pharmacol Exp Ther* **324**, 834–849.

[16] Fujio M, Yamamoto A, Ando Y, Shohara R, Kinoshita K, Kaneko T, Hibi H, and Ueda M (2011). Stromal cell-derived factor-1 enhances distraction osteogenesis-mediated skeletal tissue regeneration through the recruitment of endothelial precursors. *Bone* **49**, 693–700.

[17] Henderson PW, Singh SP, Krijgh DD, Yamamoto M, Rafii DC, Sung JJ, Rafii S, Rabbany SY, and Spector JA (2011). Stromal-derived factor-1 delivered *via* hydrogel drug-delivery vehicle accelerates wound healing *in vivo*. *Wound Repair Regen* **19**, 420–425.

[18] Tysseling VM, Mithal D, Sahni V, Birch D, Jung H, Belmadani A, Miller RJ, and Kessler JA (2011). SDF1 in the dorsal corticospinal tract promotes CXCR4+ cell migration after spinal cord injury. *J Neuroinflammation* **8**, 16.

[19] Shin JW, Lee JK, Lee JE, Min WK, Schuchman EH, Jin HK, and Bae JS (2011). Combined effects of hematopoietic progenitor cell mobilization from bone marrow by granulocyte colony stimulating factor and AMD3100 and chemotaxis into the brain using stromal cell-derived factor-1α in an Alzheimer's disease mouse model. *Stem Cells* **29**, 1075–1089.

[20] Yamaguchi J, Kusano KF, Masuo O, Kawamoto A, Silver M, Murasawa S, Bosch-Marce M, Masuda H, Losordo DW, and Isner JM, et al (2003). Stromal cell–derived factor-1 effects on *ex vivo* expanded endothelial progenitor cell recruitment for ischemic neovascularization. *Circulation* **107**, 1322–1328.

[21] Ehtesham M, Kabos P, Kabosova A, Neuman T, Black KL, and Yu JS (2002). The use of interleukin 12-secreting neural stem cells for the treatment of intracranial glioma. *Cancer Res* **62**, 5657–5663.

[22] Kish PE, Blaivas M, Strawderman M, Muraszko KM, Ross DA, Ross BD, and McMahon G (2001). Magnetic resonance imaging of ethyl-nitrosourea-induced rat gliomas: a model for experimental therapeutics of low-grade gliomas. *J Neurooncol* **53**, 243–257.

[23] Jang T, Litofsky NS, Smith TW, Ross AH, and Recht LD (2004). Aberrant nestin expression during ethylnitrosourea-(ENU)-induced neurocarcinogenesis. *Neurobiol Dis* **15**, 544–552.

[24] Jang T, Savarese T, Low HP, Kim S, Vogel H, Lapointe D, Duong T, Litofsky NS, Weimann JM, and Ross AH, et al (2006). Osteopontin expression in intratumoral astrocytes marks tumor progression in gliomas induced by prenatal exposure to *N*-ethyl-*N*-nitrosourea. *Am J Pathol* **168**, 1676–1685.

[25] Carpentier PA and Palmer TD (2009). Immune influence on adult neural stem cell regulation and function. *Neuron* **64**, 79–92.

[26] Bachoo RM, Maher EA, Ligon KL, Sharpless NE, Chan SS, You MJ, Tang Y, DeFrances J, Stover E, and Weissleder R, et al (2002). Epidermal growth factor receptor and *Ink4a/Arf*: convergent mechanisms governing terminal differentiation and transformation along the neural stem cell to astrocyte axis. *Cancer Cell* **1**, 269–277.

[27] Pike-Overzet K, van der Burg M, Wagemaker G, van Dongen JJ, and Staal FJ (2007). New insights and unresolved issues regarding insertional mutagenesis in X-linked SCID gene therapy. *Mol Ther* **15**, 1910–1916.

[28] Woods NB, Bottero V, Schmidt M, von Kalle C, and Verma IM (2006). Gene therapy: therapeutic gene causing lymphoma. *Nature* **440**, 1123.

[29] Kraitchman DL, Gilson WD, and Lorenz CH (2008). Stem cell therapy: MRI guidance and monitoring. *J Magn Reson Imaging* **27**, 299–310.

[30] Waerzeggers Y, Monfared P, Viel T, Winkeler A, and Jacobs AH (2010). Mouse models in neurological disorders: applications of non-invasive imaging. *Biochim Biophys Acta* **1802**, 819–839.

[31] Luskin MB, Zigova T, Soteres BJ, and Stewart RR (1997). Neuronal progenitor cells derived from the anterior subventricular zone of the neonatal rat forebrain continue to proliferate *in vitro* and express a neuronal phenotype. *Mol Cell Neurosci* **8**, 351–366.

[32] Ferrari D, Binda E, De Filippis L, and Vescovi AL (2010). Isolation of neural stem cells from neural tissues using the neurosphere technique. *Curr Protoc Stem Cell Biol* **15**, 2D.6.1–2D.6.18.

[33] Glass R, Synowitz M, Kronenberg G, Walzlein JH, Markovic DS, Wang LP, Gast D, Kiwit J, Kempermann G, and Kettenmann H (2005). Glioblastoma-induced attraction of endogenous neural precursor cells is associated with improved survival. *J Neurosci* **25**, 2637–2646.

[34] Amariglio N, Hirshberg A, Scheithauer BW, Cohen Y, Loewenthal R, Trakhtenbrot L, Paz N, Koren-Michowitz M, Waldman D, and Leider-Trejo L, et al (2009). Donor-derived brain tumor following neural stem cell transplantation in an ataxia telangiectasia patient. *PLoS Med* **6**, e1000029.

[35] Keene CD, Chang RC, Leverenz JB, Kopyov O, Perlman S, Hevner RF, Born DE, Bird TD, and Montine TJ (2009). A patient with Huntington's disease and long-surviving fetal neural transplants that developed mass lesions. *Acta Neuropathol* **117**, 329–338.

[36] Assanah M, Lochhead R, Ogden A, Bruce J, Goldman J, and Canoll P (2006). Glial progenitors in adult white matter are driven to form malignant gliomas by platelet-derived growth factor-expressing retroviruses. *J Neurosci* **26**, 6781–6790.

[37] Lim DA, Cha S, Mayo MC, Chen MH, Keles E, VandenBerg S, and Berger MS (2007). Relationship of glioblastoma multiforme to neural stem cell regions predicts invasive and multifocal tumor phenotype. *Neuro Oncol* **9**, 424–429.

[38] Young GS, Macklin EA, Setayesh K, Lawson JD, Wen PY, Norden AD, Drappatz J, and Kesari S (2011). Longitudinal MRI evidence for decreased survival among periventricular glioblastoma. *J Neurooncol* **104**, 261–269.

[39] Lieu AS, Hwang SL, Howng SL, and Chai CY (1999). Brain tumors with hemorrhage. *J Formos Med Assoc* **98**, 365–367.

[40] Gruszkiewicz J, Doron Y, Gellei B, and Peyser E (1969). Massive intracerebral bleeding due to supratentorial meningioma. *Neurochirurgia* **12**, 107–111.

[41] Zhang J, Sarkar S, and Yong VW (2005). The chemokine stromal cell derived factor-1 (CXCL12) promotes glioma invasiveness through MT2-matrix metalloproteinase. *Carcinogenesis* **26**, 2069–2077.

[42] Kryczek I, Lange A, Mottram P, Alvarez X, Cheng P, Hogan M, Moons L, Wei S, Zou L, and Machelon V, et al (2005). CXCL12 and vascular endothelial growth factor synergistically induce neoangiogenesis in human ovarian cancers. *Cancer Res* **65**, 465–472.

[43] do Carmo A, Patricio I, Cruz MT, Carvalheiro H, Oliveira CR, and Lopes MC (2010). CXCL12/CXCR4 promotes motility and proliferation of glioma cells. *Cancer Biol Ther* **9**, 56–65.

[44] McCandless EE, Piccio L, Woerner BM, Schmidt RE, Rubin JB, Cross AH, and Klein RS (2008). Pathological expression of CXCL12 at the blood-brain barrier correlates with severity of multiple sclerosis. *Am J Pathol* **172**, 799–808.

[45] Zhu B, Xu D, Deng X, Chen Q, Huang Y, Peng H, Li Y, Jia B, Thoreson WB, and Ding W, et al (2012). CXCL12 enhances human neural progenitor cell survival through a CXCR7- and CXCR4-mediated endocytotic signaling pathway. *Stem Cells* **30**, 2571–2583.

[46] Peng H, Huang Y, Rose J, Erichsen D, Herek S, Fujii N, Tamamura H, and Zheng J (2004). Stromal cell-derived factor 1-mediated CXCR4 signaling in rat and human cortical neural progenitor cells. *J Neurosci Res* **76**, 35–50.

[47] Lazarini F, Casanova P, Tham TN, De Clercq E, Arenzana-Seisdedos F, Baleux F, and Dubois-Dalcq M (2000). Differential signalling of the chemokine receptor CXCR4 by stromal cell-derived factor 1 and the HIV glycoprotein in rat neurons and astrocytes. *Eur J Neurosci* **12**, 117–125.

[48] Bajetto A, Barbero S, Bonavia R, Piccioli P, Pirani P, Florio T, and Schettini G (2001). Stromal cell-derived factor-1α induces astrocyte proliferation through the activation of extracellular signal-regulated kinases 1/2 pathway. *J Neurochem* **77**, 1226–1236.

[49] Kokovay E, Goderie S, Wang Y, Lotz S, Lin G, Sun Y, Roysam B, Shen Q, and Temple S (2010). Adult SVZ lineage cells home to and leave the vascular niche *via* differential responses to SDF1/CXCR4 signaling. *Cell Stem Cell* **7**, 163–173.

[50] Salcedo R and Oppenheim JJ (2003). Role of chemokines in angiogenesis: CXCL12/SDF-1 and CXCR4 interaction, a key regulator of endothelial cell responses. *Microcirculation* **10**, 359–370.

[51] Kukreja P, Abdel-Mageed AB, Mondal D, Liu K, and Agrawal KC (2005). Up-regulation of CXCR4 expression in PC-3 cells by stromal-derived factor-1α (CXCL12) increases endothelial adhesion and transendothelial migration: role of MEK/ERK signaling pathway–dependent NF-κB activation. *Cancer Res* **65**, 9891–9898.

[52] Teng H, Zhang ZG, Wang L, Zhang RL, Zhang L, Morris D, Gregg SR, Wu Z, Jiang A, and Lu M, et al (2008). Coupling of angiogenesis and neurogenesis in cultured endothelial cells and neural progenitor cells after stroke. *J Cereb Blood Flow Metab* **28**, 764–771.

[53] Allport JR, Shinde Patil VR, and Weissleder R (2004). Murine neuronal progenitor cells are preferentially recruited to tumor vasculature *via* $\alpha_4$-integrin and SDF-1α-dependent mechanisms. *Cancer Biol Ther* **3**, 838–844.

[54] Ehtesham M, Yuan X, Kabos P, Chung NH, Liu G, Akasaki Y, Black KL, and Yu JS (2004). Glioma tropic neural stem cells consist of astrocytic precursors and their migratory capacity is mediated by CXCR4. *Neoplasia* **6**, 287–293.

[55] Brown AB, Yang W, Schmidt NO, Carroll R, Leishear KK, Rainov NG, Black PM, Breakefield XO, and Aboody KS (2003). Intravascular delivery of neural stem cell lines to target intracranial and extracranial tumors of neural and non-neural origin. *Hum Gene Ther* **14**, 1777–1785.

[56] Fears CY, Sontheimer HW, Bullard DC, and Gladson CL (2004). Could labeled neuronal progenitor cells be used to target glioma tumor endothelium? *Cancer Biol Ther* **3**, 845–846.

[57] Zhao D, Najbauer J, Garcia E, Metz MZ, Gutova M, Glackin CA, Kim SU, and Aboody KS (2008). Neural stem cell tropism to glioma: critical role of tumor hypoxia. *Mol Cancer Res* **6**, 1819–1829.

[58] Shah K, Hingtgen S, Kasmieh R, Figueiredo JL, Garcia-Garcia E, Martinez-Serrano A, Breakefield X, and Weissleder R (2008). Bimodal viral vectors and *in vivo* imaging reveal the fate of human neural stem cells in experimental glioma model. *J Neurosci* **28**, 4406–4413.

[59] van Eekelen M, Sasportas LS, Kasmieh R, Yip S, Figueiredo JL, Louis DN, Weissleder R, and Shah K (2010). Human stem cells expressing novel TSP-1 variant have anti-angiogenic effect on brain tumors. *Oncogene* **29**, 3185–3195.

[60] Svendsen CN, Skepper J, Rosser AE, ter Borg MG, Tyres P, and Ryken T (1997). Restricted growth potential of rat neural precursors as compared to mouse. *Brain Res Dev Brain Res* **99**, 253–258.

[61] Svendsen CN, ter Borg MG, Armstrong RJ, Rosser AE, Chandran S, Ostenfeld T, and Caldwell MA (1998). A new method for the rapid and long term growth of human neural precursor cells. *J Neurosci Methods* **85**, 141–152.

[62] Khan MZ, Brandimarti R, Shimizu S, Nicolai J, Crowe E, and Meucci O (2008). The chemokine CXCL12 promotes survival of postmitotic neurons by regulating Rb protein. *Cell Death Differ* **15**, 1663–1672.

[63] Opatz J, Küry P, Schiwy N, Järve A, Estrada V, Brazda N, Bosse F, and Müller HW (2009). SDF-1 stimulates neurite growth on inhibitory CNS myelin. *Mol Cell Neurosci* **40**, 293–300.

[64] Pujol F, Kitabgi P, and Boudin H (2005). The chemokine SDF-1 differentially regulates axonal elongation and branching in hippocampal neurons. *J Cell Sci* **118**, 1071–1080.

[65] Rodriguez FJ, Scheithauer BW, Robbins PD, Burger PC, Hessler RB, Perry A, Abell-Aleff PC, and Mierau GW (2007). Ependymomas with neuronal differentiation: a morphologic and immunohistochemical spectrum. *Acta Neuropathol* **113**, 313–324.

[66] Varlet P, Soni D, Miquel C, Roux FX, Meder JF, Chneiweiss H, and Daumas-Duport C (2004). New variants of malignant glioneuronal tumors: a clinicopathological study of 40 cases. *Neurosurgery* **55**, 1377–1391 [discussion 1391–1392].

[67] Donev K, Scheithauer BW, Rodriguez FJ, and Jenkins S (2010). Expression of diagnostic neuronal markers and outcome in glioblastoma. *Neuropathol Appl Neurobiol* **36**, 411–421.